ACCSCIENCE PUBLISHING

Advanced Neurology

ORIGINAL RESEARCH ARTICLE

Metabolomic profiling of aluminum chloride-intoxicated rats treated with novel dual inhibitors targeting acetylcholinesterase for Alzheimer's therapy

Samir H. I. Haggag, Noha S. Hussein, Abdel-Hamid Z. Abdel-Hamid, Hanan F. Aly*, Eman A. Younis, Asmaa F. Aboul-Naser, and Maha Z. Rizk

Department of Therapeutic Chemistry, Pharmaceutical Industries Research Institute, National Research Centre, Dokki, Cairo, Egypt

Abstract

Millions of elderly people worldwide have Alzheimer's disease (AD), a complex and progressive neurological illness. AD can only be definitively diagnosed postmortem by examining brain tissue obtained during autopsy, which makes detection and intervention challenging. Therefore, identifying specific metabolites as potential metabolic biomarkers associated with AD risk is crucial. For a comprehensive understanding of the role of metabolic biomarkers in AD etiology, we performed metabolomics-based gas chromatography–mass spectrometry to characterize serum metabolite alterations in rats with $AlCl_3$-induced AD-like neurotoxicity. We evaluated metabolite levels across five experimental groups (10 rats per group). We further conducted metabolic profiling to identify metabolomic features associated with AD risk and to assess the therapeutic effects of newly synthesized compounds, including benzofuran-derivative-7 (MP19) and coumarin-3 (MP27). Four metabolites identified in this study provided strong discriminative power for AD diagnosis, offering a potential approach for biomarker detection that may enhance patient diagnosis and prognosis in the future. This study provides new insights into the etiology, early detection, and potential therapy for AD, involving blood-based metabolic biomarkers that warrant further investigation.

Keywords: Alzheimer; Metabolomics; Gas chromatography–mass spectrometry; Metabolic biomarkers; Benzofuran; Coumarin derivatives

***Corresponding author:**
Hanan F. Aly
(hanan_abduallah@yahoo.com)

Citation: Haggag SHI, Hussein NS, Abdel-Hamid AHZ, *et al*. Metabolomic profiling of aluminum chloride-intoxicated rats treated with novel dual inhibitors targeting acetylcholinesterase for Alzheimer's therapy. *Adv Neurol*. 2026;5(4):025510129. doi: 10.36922/AN025510129

Received: December 20, 2025

Revised: March 25, 2026

Accepted: April 1, 2026

Published online: May 12, 2026

Copyright: © 2026 Author(s). This is an Open-Access article distributed under the terms of the Creative Commons Attribution License, permitting distribution, and reproduction in any medium, provided the original work is properly cited.

Publisher's Note: AccScience Publishing remains neutral with regard to jurisdictional claims in published maps and institutional affiliations.

1. Introduction

Dementia is a clinical syndrome that primarily affects the elderly.[1] One of the primary types of dementia, Alzheimer's disease (AD), is characterized by a progressive decline in cholinergic neurotransmission, which leads to brain dysfunction, loss of reasoning, communication, or learning abilities. It is also characterized by memory loss and neuropsychiatric symptoms, along with progressive impairment in behavioral and daily functioning.[2] AD and other neurological conditions cause progressive and permanent neuronal deterioration, which leads to the loss of cognitive abilities.[3] The World Health Organization also projected a future increase in the number of patients

with neurodegenerative diseases.[4] Although the exact sequences of these events are unknown, the formation of neurofibrillary tangles by hyperphosphorylated tau protein, the amyloid-β hypothesis, and the cholinergic hypothesis are key pathological features of brain injury in AD. The primary cause of AD is the reduction of acetylcholine, which is associated with increased acetylcholinesterase (AChE) activity and alterations in neurotransmitter synthesis and levels in the brain, leading to progressive cognitive impairment[5]

There is currently no cure for senile dementia due to its complex etiology, gradual progression, hidden course, and other features.[6] There are several signaling pathways involved in the intricate pathophysiology of AD; however, the precise cause of AD remains unknown.[7] Metabolomics serves as a promising new method for comprehending the biology of dementia and identifying biomarkers for dementia risk.[8] Metabolomics can also be used to monitor therapy response and disease progression, as well as to discover biomarkers for early AD diagnosis and new therapeutic targets.[9]

Additionally, given the similarities between human and experimental animal metabolisms, metabolomics offers a convenient way to facilitate the translation of findings from animal models to human studies and may support drug-development efforts.[9] Investigating the role of metabolism in AD pathogenesis can be facilitated by large-scale metabolomics approaches, which may help provide a more thorough understanding of AD pathology and the underlying processes of disease symptoms.[10] Currently, little is known about the metabolic factors that underlie AD pathology and the ensuing cognitive loss in AD.[11-13]

A polypharmacological strategy based on the creation of a single molecular entity, such as coumarins, intended to concurrently modulate multiple validated biological targets, could improve current therapies, which are largely symptomatic. This approach primarily relies on molecular hybridization, which involves combining several chemical moieties through complementary or synergistic interactions. Benzofuran (BF) derivatives have shown promise as neurotherapeutic agents and were therefore considered as candidate scaffolds in the present study.

Our research team has recently identified nitrogen-containing heterocyclic compounds, such as indole and benzimidazole derivatives, as potential therapeutic agents for AD.[14-16] AChE inhibition was assessed in all analogs using donepezil, a common medication, as a positive control. Numerous bioactive natural and synthetic heterocyclic compounds contain the BF scaffold; these compounds exhibit a wide range of biological activities, such as anti-inflammatory effects, AChE inhibitory activity, and blood–brain barrier permeability. Since the naturally occurring BF scaffold can be considered a structural mimic of the indanone moiety of donepezil, compounds generated from BF have shown potential in the development and identification of neurotherapeutic agents. Therefore, the design and synthesis of BF-based compounds could provide a valuable library of molecules to explore the multitarget potential of this scaffold, thereby facilitating the development of potent anti-AD therapeutics.

Additionally, the coumarin scaffold (2H-1-benzopyran-2-one) exhibits a range of biological functions, and its multiple sites for chemical substitution[14] make coumarins attractive candidates for drug development, particularly as AChE inhibitors. Coumarin scaffolds also demonstrated the capacity to influence several pathological pathways and targets, such as AChE, butyrylcholinesterase, beta-site amyloid precursor protein cleaving enzyme 1, cyclooxygenase-2, lipoxygenase, cannabinoid receptors, fatty acid amide hydrolase enzyme, gamma-aminobutyric acid receptors, and monoamine oxidases, all of which are thought to be implicated in the pathogenic mechanisms of AD. It is most likely connected to the production of harmful byproducts during catalyzed metabolic reactions, specifically aldehydes, ammonia, and hydrogen peroxide.

Based on preliminary docking studies, we designed and synthesized a series of BF and coumarin compounds as analogs of the reference drug donepezil. The compounds were synthesized and evaluated for their AChE inhibitory activity, and from each series, the most promising molecule was chosen. The chemical synthesis, analytical information, and docking studies of these compounds were conducted in compliance with previous publications.[13]

Previous studies[14-16] demonstrated that both benzofuran-derivative-7 (BF-7; MP19) and coumarin-3 (Cou-3; MP27) were selected over other analogs due to their superior inhibitory activity compared to the standard drug, donepezil. Furthermore, MP19 and MP27 showed inhibitory activity with half-inhibitory concentrations of 0.058 μg/mL[15] and 0.0802 μg/mL,[16] respectively, compared to donepezil (0.049 μg/mL).[17]

Since aluminum is associated with the development of numerous neurological disorders, including AD, the current study used aluminum chloride ($AlCl_3$) to generate AD-like dementia in rat models. Aluminum accumulation in the brains of test animals is believed to compromise the blood–brain barrier, thereby increasing the risk of neurological damage. This occurs because aluminum can induce brain damage,[17] disrupt brain neurochemistry, damage brain DNA, and interfere with the action of antioxidant enzymes.[18] Chronic aluminum exposure has

been shown to cause neurological signs and symptoms that closely resemble advanced neurodegeneration. Additionally, aluminum-induced AD in animal models has been associated with neurofilament abnormalities and metabolic alterations in the hippocampus and cerebral cortex.[18]

The present study examined the metabolomic profiles of the sera of rats intoxicated with $AlCl_3$ and administered a BF derivative, namely, 3-((3-acetylphenyl) amino)-1-(benzofuran-2-yl) prop-2-en-1-one, and a coumarin derivative, namely, N'-(2,3-dihydro-1H-inden-1-ylidene)-2-((4-methyl-2-oxo-2H-chromen-7-l)oxy)acetohydrazide, known as MP19 and MP27, respectively. These molecules were administered to identify metabolites that could serve as potential novel biomarkers against brain neurodegeneration.

2. Materials and methods

2.1. Chemical analyses

Chemical analyses, namely melting points, elemental microanalyses, infrared spectra, and ^{1}H and ^{13}C nuclear magnetic resonance spectra, were evaluated at the National Research Centre, Cairo, and the Faculty of Pharmacy, Cairo University, Egypt. MP19 and MP27 were synthesized as previously reported.[14-16]

2.2. Drugs and chemicals

Aluminum chloride, methoxamine hydrochloride, pyridine, N-methyl-N (trimethylsilyl) trifluoroacetamide (MSTFA) with 1% (vol/vol) trimethylchlorosilane, methyl-tert butyl ether, methanol (high-performance liquid chromatography grade), and n-alkane C8–C40 standard were purchased from Sigma-Aldrich (United States).

2.3. Animals and experimental design

Based on our previous toxicity study, the dosage of the test substance was selected with reference to standard medications, specifically donepezil at 10 mg/kg body weight per day.[19]

2.3.1. Aluminum chloride-induced Alzheimer's disease rat model

Aluminum chloride solutions were prepared freshly in distilled water immediately before use and were given daily for two months to rats orally at a dosage of 100 mg/kg/day (0.5 mL per day).[19] Fifty mature male Wistar rats weighing 200 ± 30 g were acquired from the National Research Centre animal house in Egypt. Rats were allowed free access to food and water and kept in housing with light/dark cycles of 12 hours (7:00 a.m. to 7:00 p.m.). Following two weeks of acclimatization, the rats (n = 10) were split into five groups at random as follows:

(i) Group I: Negative control group. Rats were given distilled water orally as a vehicle.
(ii) Group II: $AlCl_3$-induced AD rats. Rats were administered $AlCl_3$ intragastrically at a dose of 100 mg/kg body weight for eight weeks.
(iii) Group III: AD + MP19-treated group. Rats were given $AlCl_3$ for eight weeks. Treatment was started immediately with MP19 (10 mg/kg body weight/day) intragastrically for six weeks.
(iv) Group IV: AD + MP27-treated group. Rats were given $AlCl_3$ for eight weeks and then intra-gastric administration of MP27 (10 mg/kg body weight/day) for six weeks.
(v) Group V: AD + donepezil-treated group. Rats were given $AlCl_3$ for eight weeks before receiving intragastric administration of donepezil (10 mg/kg body) for six weeks.[14]

2.3.2. Blood sampling

After $AlCl_3$ intoxication and subjection to both treatments, blood was drawn from the orbital plexus of the eyes, collected, and centrifuged using a bench-top centrifuge (Hettich, Germany) at 4,000 rpm for 10 min. To completely remove cellular components, the supernatant was separated and centrifuged at 13,000 rpm, using a cooling centrifuge at 4 °C for 10 min (Sigma-Aldrich, Germany). Samples were stored at −80 °C until further use.

2.4. Ethics and permissions

All procedures were designed in accordance with the ethical principles for medical research involving animal subjects. The study protocol was ethically reviewed and approved by the Ethics Review Committee of the National Research Center in Cairo (Approval no: 12010114).

2.5. Serum metabolome analysis using gas chromatography–mass spectrometry

The extraction of metabolites from serum samples was conducted in accordance with the method described by Ammar *et al.*[20] For serum gas chromatography–mass spectrometry (Turbomass, United States) analysis, 100 µL of serum was mixed with 200 µL of cold acetonitrile (100%) containing 5 µL xylitol (1 mg/mL, internal standard) and centrifuged at 11,000 × g for 15 min to precipitate the proteins. After centrifugation, the supernatant was dried using a nitrogen dryer. For metabolite derivatization, 50 µL of methoxyamine hydrochloride dissolved in 20 mg/mL pyridine was added to the dried pellet, which was then incubated at 60 °C for two hours. In the second derivatization step, 100 µL of MSTFA containing 1% trimethylchlorosilane was added to the mixture and incubated at 60 °C for one hour.

2.6. Gas chromatography–mass spectrometry analysis conditions

A Trace Ultra Gas Chromatograph (Thermo Scientific Corp., United States) coupled to a mass spectrometer detector (ISQ Single Quadrupole Mass Spectrometer; PerkinElmer, United States) was used to analyze serum metabolites. Chromatographic separation was achieved on a TG-5MS column (30 m × 0.25 mm i.d., 0.25 µm film thickness) to analyze derivatized serum samples. Analysis was carried out using helium as the carrier gas at a flow rate of 1.0 mL/min and a split ratio of 1:10 using the following temperature program: 80 °C for two minutes; rising at 5 °C/min to 300 °C and held for five minutes. The injector and detector were held at 280 °C. Mass spectra were obtained by electron ionization at 70 eV, using a spectral range of *m/z* 35–500.

For data preprocessing, we used XCMS (version 3.23) and MZmine (version 3.9.0). Data processing was performed in three steps: (i) peak picking: this step identifies individual ion signals in each sample by separating them from background noise; (ii) alignment (correspondence): this step accounts for variations in retention time and mass-to-charge ratio (*m/z*) across different samples or batches to ensure that the same metabolite is grouped correctly; and (iii) filtering and refinement: this step removes low-quality features, artifacts, or redundant signals to improve downstream statistical power.

For metabolite identification, the detected mass spectra were deconvoluted and matched against reference libraries from Wiley and the National Institute of Standards and Technology to identify measured peaks based on similarity to previously registered reference compounds. Standard fatty acid mixture (Sigma-Aldrich, United States) was injected to confirm peak assignments. Retention indices were calculated relative to n-alkanes (C8–C40) standards.[21]

2.7. Data processing for multivariate analysis

The multivariate analysis of identified metabolites was performed using MetaboAnalyst 6.0, a comprehensive tool for metabolic data analysis (http://www. metaboanalyst. ca).[22] Metabolites' mass spectrometry signals were normalized using the reference sample feature. Data transformation was performed using log transformation, specifically the Pareto scaling option, prior to multivariate data analysis. Subsequently, both unsupervised principal component analysis and supervised partial least squares-discriminant analysis (PLS-DA) were performed using this program.[23]

2.8. Statistical analysis

Nonparametric tests (Mann–Whitney and Kruskal–Wallis) were conducted using Statistical Package for the Social Sciences version 17, and $p \leq 0.05$ was considered significant. Additionally, we performed a permutation and accuracy test using MetaboAnalyst (version 6.0) to assess the model's fit, yielding $p \leq 0.05$, confirming stability. Metabolites contributing to group segregation were identified from the variable importance in projection (VIP) plot of the PLS-DA model (VIP score ≥ 1) to determine the key metabolites and their concentrations in each studied group.

Analysis of variance was performed for all metabolites using the Statistical Package for Social Sciences (version 6.0) and MetaboAnalyst 6.0 software, with post hoc analysis (Fisher's least significant difference) and *p*-value ≤ 0.05. A classical ROC curve using the MetaboAnalyst 6.0 software was performed using the area under the curve (AUC) values.

3. Results

3.1. Profiling of serum metabolites using multivariate data analytics and gas chromatography–mass spectrometry analysis

Serum metabolites were efficiently extracted, isolated, and analyzed using gas chromatography–mass spectrometry. A total of 31 metabolites, including sugars, free fatty acids, sterols, and organic acids, were identified, as shown in Table 1.

For a multivariate statistical method for discriminant analysis, principal component analysis and supervised PLS-DA models were constructed from metabolomics profiling data obtained from the healthy (–), AD (+), and treated groups, as shown in Figure 1A and 1B, respectively. The first two principal components (PC), namely PC1 (41.8%) and PC2 (31.4%), were obtained from the PLS-DA model. The AD group displayed clear separation from the healthy and other groups along PC1. The model parameters, R^2 and Q^2 (cumulative), were 0.78 and 0.59, respectively, indicating acceptable fitting and predictive power. These results suggest that the PLS-DA model is reliable and suitable for identifying potential AD biomarkers. Additionally, we performed a permutation test and an accuracy test to assess the model's fit, yielding $p \leq 0.05$, confirming its stability (Figure 2A and 2B).

Metabolites contributing to group segregation were identified from the VIP plot of the PLS-DA model (VIP score ≥ 1) to determine the key metabolites and their concentrations in each studied group (Figure 1D). These metabolites included octadecanoic acid (stearic acid), hexadecanoic acid (palmitic acid), galactose, oleic acid, and glucose. The levels of these metabolites in rats' sera varied

Table 1. Serum metabolites derived from gas chromatography-mass spectrometry

Retention time (min)	Compounds	Control	Positive control	Reference drug	MP27	MP19
5.71	Propanoic acid, 2-[(trimethylsilyl)oxy]-, trimethylsilyl ester	0.75	0.59	0.46	0.44	0.45
6.04	Glycine, N,N-bis(trimethylsilyl)-, methyl ester	0.64	0.69	0.80	0.67	0.58
7.89	Ethanedioic acid, bis(trimethylsilyl) ester	2.50	2.33	2.25	3.25	2.35
8.19	Butanoic acid, 3-[(trimethylsilyl)oxy]-, trimethylsilyl ester	8.59	8.85	8.25	8.70	9.12
8.65	Pentasiloxane, dodecamethyl-	0.28	0.41	0.28	0.47	0.22
9.38	Naphthalene (2,3-dimethyl-1-(trimethylsilyl))	1.29	1.56	1.40	1.73	1.57
9.85	Urea, N,N'-bis(trimethylsilyl)	4.65	3.50	4.04	10.29	1.43
11.41	Silanol, trimethyl-, phosphate (3:1)	4.04	4.65	3.75	5.60	4.35
14.2	Phenol, 2,4-bis(1,1-dimethylethyl)-	1.15	1.21	1.36	1.25	1.01
16.74	Xylitol, 1,2,3,4,5-pentakis-O-(trimethylsilyl)	6.39	6.99	3.25	2.91	1.50
18.28	Galactose,1,2,3,5,6-pentakis-O-(trimethylsilyl)-	1.84	12.51	7.08	11.45	10.24
18.81	Galactopyranose	0.76	0.78	0.71	1.10	0.64
19.71	D-Glucose	9.28	13.13	10.76	12.38	11.23
20.06	Hexadecanoic acid, trimethylsilyl ester	1.86	15.94	3.95	15.00	11.26
20.44	Oleanitrile	4.80	5.05	5.85	0.63	4.75
21.18	Octadecanoic acid, 2,3-bis[(trimethylsilyl)oxy]propyl ester	9.92	25.12	11.00	20.82	15.87
21.71	11-cis-octadecenoic acid, trimethylsilyl ester	8.25	9.15	8.35	7.95	9.20
21.93	Oleic acid, N-trimethylsilyl-, or hexadecanoic acid, trimethylsilyl ester	6.30	3.50	5.79	3.92	4.76
23.21	D-Glucose, 2,3,4,5,6-pentakis-O-(trimethylsilyl)-, o-methyloxyme,	1.39	1.10	1.15	1.29	1.39
23.25	Octadecanamide (Z)-	1.44	0.50	1.06	1.94	2.23
23.48	Oleamide 1, N-trimethylsilyl-7-methoxy-heptanoic acid, acetyl-octadecyl-amide	10.56	18.95	9.76	8.89	9.52
23.54	Linoleic acid ethyl ester or 9-octadecenamide, 12-hydroxy-	2.27	1.85	2.50	2.00	2.40
24.12	Oleanitrile, trans-13-docosenamide, 9-hexadecenoic acid, 9-octadecenyl ester	1.00	1.05	1.30	1.09	1.70
24.66	Dinonanoin monocaprylin	7.82	3.36	7.90	4.82	2.29
24.77	Cis-11-eicosenamide trans-11-icosenamide	1.01	1.24	1.15	2.14	5.24
26.40	13-docosenamide, (Z)-N methyl	9.67	5.52	2.99	12.76	2.63
26.65	Myo-inositol,1,3,4,5,6-pentakis-o-(trimethylsilyl)-, bis(trimethylsilyl)phosphate	0.28	0.47	0.42	0.41	0.48
30.90	Hexadecanoic acid, 2,3-bis[(trimethylsilyl)oxy]propyl ester	1.17	1.52	1.55	1.30	1.35
32.60	Octadecanoic acid, 2,3-bis[(trimethylsilyl)oxy]propyl ester	0.71	0.71	0.79	1.35	0.72
34.91	Phosphorodichloridic acid, 9,10-dihydro-10-oxo-9, 9-diphenyl-1,8-anthracenediyl ester	0.90	0.92	0.85	0.78	0.89
37.95	Cholesterol trimethylsilyl ether, silane	4.23	2.27	4.40	5.05	5.21

Note: Metabolomic profiling data that were produced from healthy (−), Alzheimer's disease (+), and treated groups.

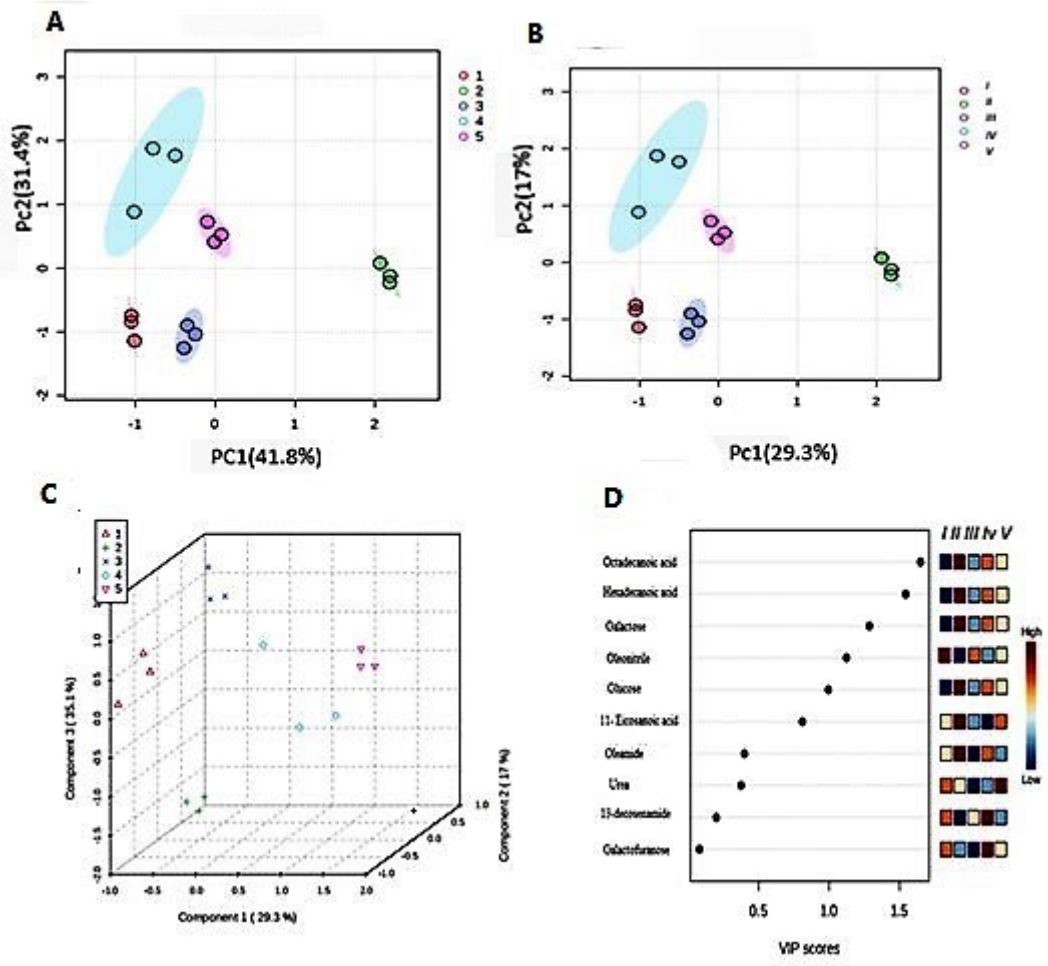

Figure 1. Plots of PLS-DA scores acquired from rats' sera gas chromatography–mass spectrometry data by modeling healthy control (I), Alzheimer's disease group (II), reference drug (V), MP27 (IV), and MP19 (III) against each other. (A, B) PC1 and PC2 score plots. (C) The three-dimensional plot shows the actual separation of the studied groups. (D) VIP score plot for key metabolite identification (VIP score ≥ 1). The relative concentrations of the related metabolites in each study group are shown by the colored boxes on the right.
Abbreviations: PC: Principal component; PLS-DA: Partial least squares-discriminant analysis; VIP: Variable importance in projection.

across all studied groups. Figure 1D shows an elevation of stearic acid, palmitic acid, galactose, and glucose, along with a decrease in oleic acid levels in Group II compared to the healthy control group (Group I). This alteration was ameliorated in the reference drug group (Group V) and the treated groups MP19 (Group III) and MP27 (Group IV), indicating that treatment with MP19 improves disease-associated metabolic changes.

The hierarchical clustering/dendrogram analysis (Figure 2) further segregated the groups and illustrated their relationships based on metabolite levels. According to this dendrogram, the normal group (Group I) was the most distant from the AD group (Group II) and other groups (standard drug and treated groups). Among the treated groups, the reference drug (Group V) and MP19 (Group III) groups were closest to the normal group, whereas the MP27 group (Group IV) remained closer to Group II, suggesting lower efficacy in disease amelioration.

Additionally, the PLS-DA model and the VIP score plot generated by it were used to identify metabolite markers associated with AD by comparing healthy controls with AD patients (Figure 3A–C). The R^2 and Q^2 values of the PLS-DA model were 0.99 and 0.98, respectively, indicating excellent discrimination between control and AD groups. In the AD group, oleic acid and 13-docosenamide were decreased, whereas glucose, galactose, hexadecanoic acid (palmitic acid), and eicosanoic acid (arachidic acid) were elevated compared to healthy controls.

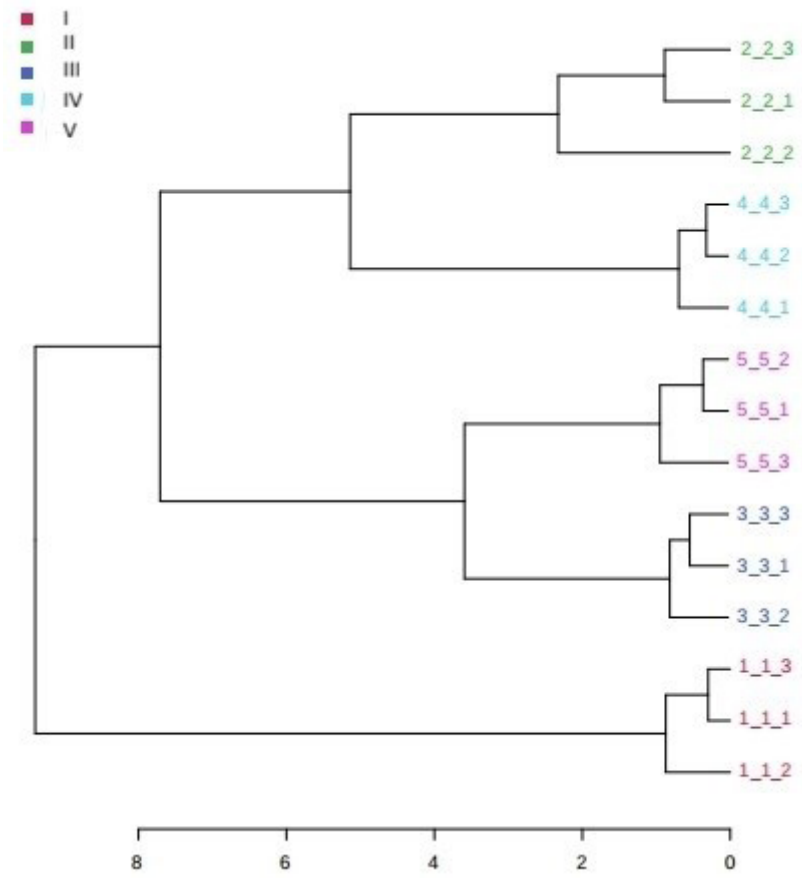

Figure 2. Hierarchical clustering/dendrograms of three rats' sera metabolites in all studied groups. The Alzheimer's disease group displayed disassociation from the normal control group in serum samples.
Note: (I) Normal control, (II) Alzheimer group, (V) Standard drug, (IV) MP27-treated group, and (III) MP19-treated group.

From multivariate analysis, common metabolites derived from VIP (PLS-DA) across all groups, including healthy and AD groups (Figure 1D), were octadecanoic acid (stearic acid), hexadecanoic acid (palmitic acid), galactose, oleic acid, glucose, and eicosanoic acid.

For the univariate analysis, analysis of variance was performed for all metabolites using the Statistical Package for Social Sciences and MetaboAnalyst 6.0 software, with post hoc analysis (Fisher's least significant difference) and *p*-value (≤0.05). The results confirmed significant differences in stearic acid, palmitic acid, galactose, oleic acid, and glucose levels (Table 2). Violin plots (Figure 4) were also generated to illustrate the significance of these metabolic biomarkers across the five groups.

From multivariate and univariate analyses of the groups under study, we indicated that hexadecanoic acid (palmitic acid), galactose, glucose, and oleic acid may serve as vital biomarkers to distinguish and diagnose AD and measure the ameliorative effect of different treatment groups by restoring these metabolites to their normal levels. To provide additional scientific evidence on these diagnostic biomarkers, we conducted a receiver operating characteristic (ROC) analysis. In this analysis, we generated a classical ROC curve using MetaboAnalyst 6.0, as shown in Figure 5. Galactose, hexadecanoic acid, glucose, and oleic acid exhibited different AUC values: 0.054 (1, 1), 0.044 (1, 1), 0.039 (1, 1), and 0.0059 (1, 1), respectively (Figure 5). These findings indicate that galactose, hexadecanoic acid, and glucose offered the highest discriminating ability for diagnosing AD.

The features identified in this analysis were ranked based on the area under the ROC curve, *t*-statistics, and $\log_2$ fold change. The results indicate that these metabolic parameters achieved AUC values of 1.0, suggesting excellent discriminatory performance. The metabolites that showed the greatest differences between AD-induced rats and normal controls are summarized in Table 3.

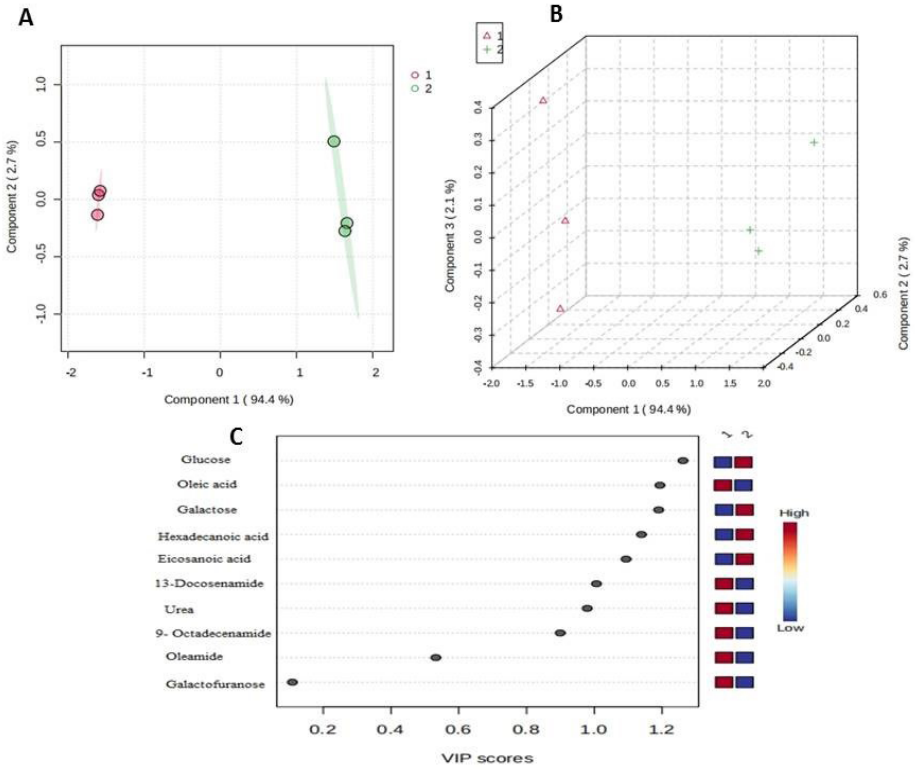

Figure 3. Plots of PLS-DA scores acquired from rats' sera gas chromatography–mass spectrometry data by modeling healthy control (I) and Alzheimer's disease group (II) against one another. (A, B) Score plot of PC1 and PC2. (C) VIP score plot for determination of key metabolites (VIP score ≥ 1): glucose (1.3), oleic acid (1.09), galactose (1.08), hexadecanoic acid (1.05), and eicosanoic acid (1.03). The relative concentrations of the related metabolites in each study group are shown by the colored boxes on the right.
Abbreviations: PC: Principal component; PLS-DA: Partial least squares-discriminant analysis; VIP: Variable importance in projection.

Table 2. The most significant biomarkers for Alzheimer's disease diagnosis

Compounds	*F*-values	*p*-values	−log *p*-values	False discovery rate
Stearic acid	1,221.0	2.13×10^{-13}	12.67	2.34×10^{-12}
Glucose	603.55	7.14×10^{-12}	11.15	3.93×10^{-11}
Oleic acid	306.52	2.06×10^{-10}	9.69	7.57×10^{-10}
Palmitic acid	134.21	1.21×10^{-8}	7.92	3.32×10^{-8}
Galactose	97.22	5.82×10^{-8}	7.23	1.28×10^{-7}

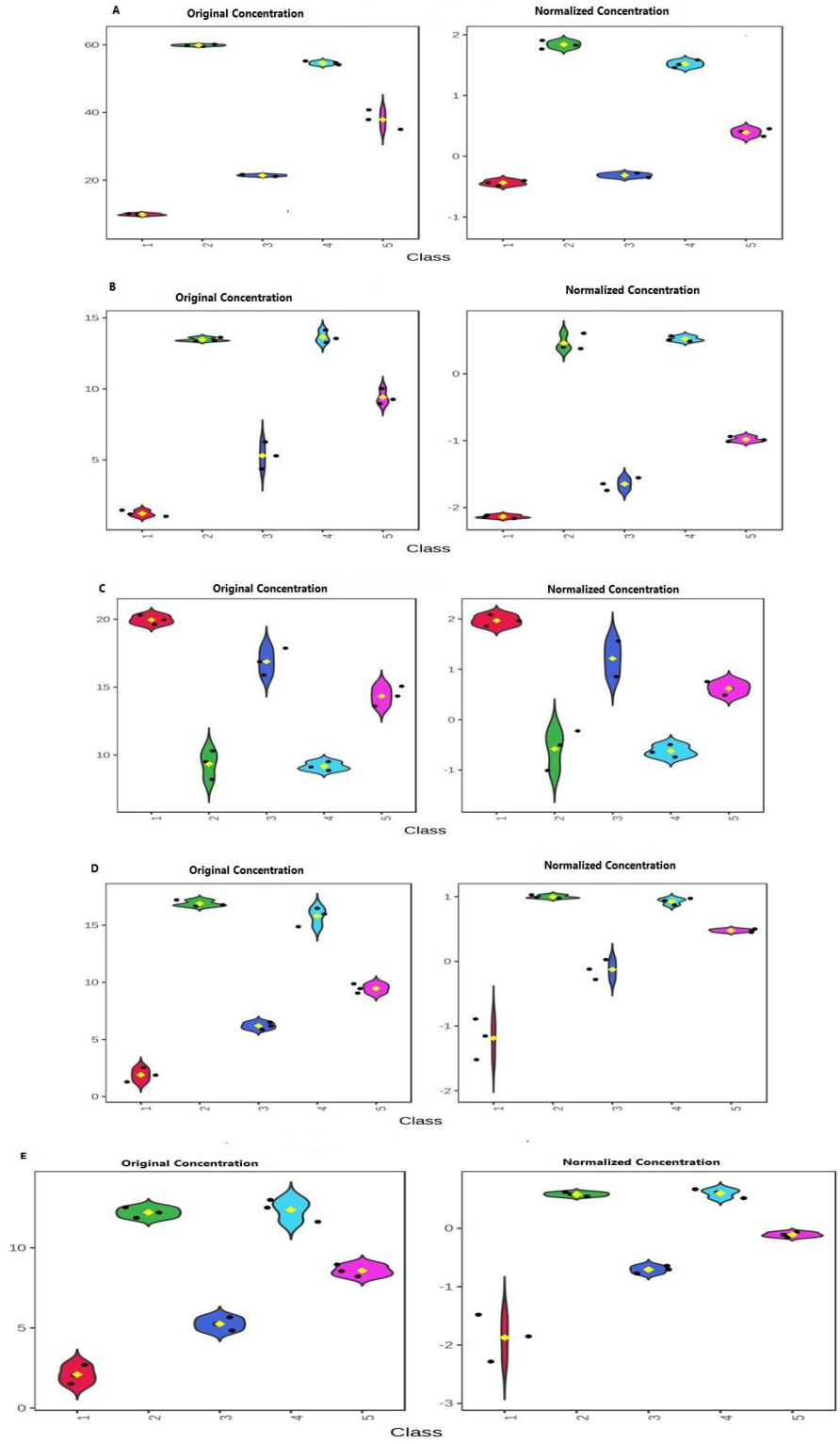

Figure 4. Violin plots showing concentrations and significant metabolic biomarkers across experimental groups. (A) Octadecanoid acid, (B) D-glucose, (C) oleic acid, (D) hexadecenoic acid, and (E) galactose.
Note: (I) Normal control, (II) Alzheimer group, (V) Standard drug, (IV) MP27-treated group, and (III) MP19-treated group.

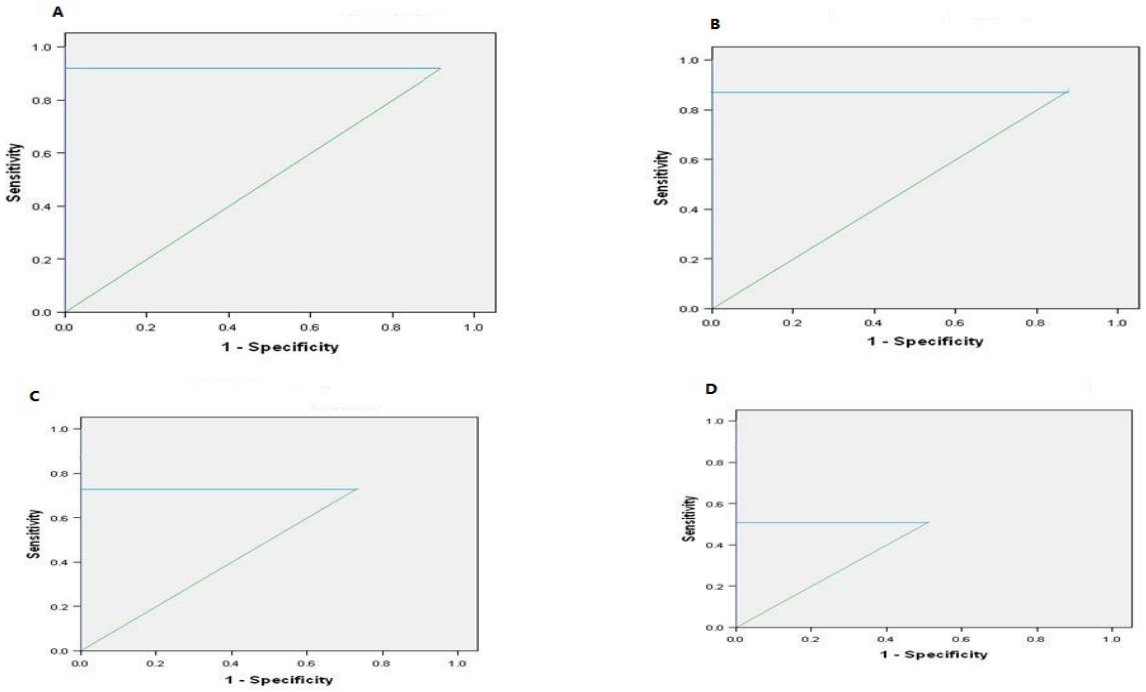

Figure 5. Receiver operating characteristic curves of (A) palmitic acid (hexadecanoic acid), (B) galactose, (C) glucose, and (D) oleic acid with different area under the curve values

According to the *p*-values of the *t*-test, the most significant biomarkers were glucose, galactose, and palmitic acid. Multivariate ROC curve analysis was also conducted to validate these findings and to evaluate the performance of biomarker models generated through automated metabolite selection. The concentrations and statistical significance of each metabolite are presented in Table 4.

4. Discussion

Globally, AD is the most common neurological illness. It is challenging to forecast when a patient will transition from the prodromal stage to dementia due to the wide variation in disease progression and the lack of comprehensive knowledge of the molecular mechanisms causing AD. We speculate that metabolic changes at the brain level may be mirrored systemically in patients' blood serum and serve as prognostic indicators.[24]

Our previous results[15] illustrated that AD rats treated with MP19 mitigated $AlCl_3$-induced neurotoxicity by improving motor function, attenuating apoptosis, and modulating cholinergic pathways. In addition, insulin 1 expression was significantly upregulated in AD-induced rats treated with BF-7.[15] Additionally, our previous results[14] showed that MP19 did not induce histopathological damage to normal liver, kidney, heart, or brain tissues. It also reduced tissue malondialdehyde levels, increased glutathione levels, and reduced the expression levels of the *App* and *Tau* genes in AD rats.

In this study, we observed elevations in three biomarkers (galactose, glucose, and palmitic acid, a saturated fatty acid) and a decrease in oleic acid (a monounsaturated fatty acid) in the Alzheimer group compared to the healthy group. The pathophysiology and course of AD profoundly affect metabolites and associated metabolic pathways, such as fatty acid and energy metabolism, as shown by metabolomic investigations.[25]

Generally, AD brains exhibit abnormalities in membrane lipids in neurogenerative diseases.[26] These conditions are linked to abnormal phospholipid metabolism resulting from a complex series of biological processes in hypoxic neurons, including glutamate release and a significant calcium influx. Consequently, pathological overactivation of catabolic enzymes is induced, principally phospholipase A2.[27] With the release of free fatty acids, this enzymatic stimulation degrades phosphatidylcholine to produce lyso-phosphatidylcholines, which quickly hydrolyze to glycerophosphocholine, phosphocholine, and ultimately choline (free fatty acids).[28]

Table 3. The common metabolites derived from the receiver operating characteristic analysis

Metabolites	Area under the curve	*p*-value	Log_2 fold change
Palmitic acid	0.91	4.682×10^{-5}	−1.79
Galactose	0.87	3.95×10^{-4}	−1.76
Glucose	0.77	5.419×10^{-6}	+3.89
Oleic acid	0.53	7.614×10^{-4}	+1.5

Table 4. The most effective biomarkers across the studied groups

Compound	Healthy control (Group I)	Alzheimer's disease (Group II)	MP19 (Group III)	MP27 (Group IV)	Reference drug (Group V)
Galactose	1.84 ± 0.60*	12.51 ± 0.37	10.24 ± 0.69*	11.45 ± 0.33	7.08 ± 0.96*
Glucose	9.28 ± 0.23*	13.13 ± 0.55	11.23 ± 0.44*	12.38 ± 0.14	10.76 ± 0.39*
Oleic acid	6.30 ± 0.45*	3.50 ± 0.43	4.76 ± 0.06*	3.92 ± 0.27	5.61 ± 0.32*
Palmitic acid	1.86 ± 0.59*	15.94 ± 0.42	11.26 ± 0.82*	15.00 ± 0.28	3.95 ± 1.00*

Notes: Data is expressed as mean ± standard deviation. * indicates that the metabolites are significant compared to the Alzheimer group at $p \leq 0.05$.

This suggests that, in addition to the overactivation of well-known membrane-destabilizing processes mediated by phospholipases, an imbalance in the ratio of saturated to unsaturated fatty acids within phospholipid structures contributes to this aberrant state, ultimately leading to cell death. Given that polyunsaturated and monounsaturated fatty acid-containing phospholipids are abundant in the easily oxidizable oleic, arachidonic, and docosahexaenoic acids, their decline may indicate a role for oxidative stress in the progressive deterioration of brain phospholipids in AD. However, as polyunsaturated fatty acids are crucial for membrane structure and permeability, their substitution with saturated fatty acids, such as palmitic acid, may contribute to the destabilization of neuronal membranes.[29,30] These facts are consistent with our experiments, which show low levels of oleic acid (a monounsaturated fatty acid) in AD and high levels of palmitic acid (a saturated fatty acid). Consequently, it has been shown that blood serum samples can be used to examine these alterations in brain chemistry.[29]

Palmitic acid is a saturated fatty acid that has been linked to the development of type II diabetes and obesity. It is yet unknown how high neuronal palmitic acid levels and higher expression of AD markers are related. Among other effects, González-Domínguez *et al.*[30] reported that palmitic acid decreases the activity of the deacetylase sirtuin1 in neurons by causing insulin resistance, raising intracellular calcium and reactive oxygen species generation, and decreasing the nicotinamide adenine dinucleotide+/ reduced nicotinamide adenine dinucleotide ratio. These processes could affect signaling pathways that regulate post-translational modifications of the tau protein. Several AD-related sites, including S199/202 and S214, exhibited altered phosphorylation states driven by dysregulated activity of the kinases mammalian target of rapamycin and glycogen synthase kinase-3 beta. Prolonged exposure to

palmitic acid also increased total tau levels and enhanced acetylation at residue K280. These findings provide insight into the mechanisms by which saturated fatty acids induce tau post-translational modifications and mirror biochemical alterations observed in AD.[31]

The brain has exceptionally high energy demands, relying primarily on glucose (and, under certain conditions, galactose), as neurons have limited energy reserves and depend on a continuous supply of circulating substrates. Oxidative phosphorylation serves as the primary energy source for maintaining ion gradients across the plasma membrane. However, AD causes a decrease in brain glucose metabolic rate due to depletion of energy-generating metabolism[32] and mitochondrial dysfunction.

However, this aberrant energy metabolism has also been linked to reduced levels of creatine and carnitine. Through the creatine kinase/phosphocreatine system, which facilitates the movement of energy from mitochondria to the cytosol, creatine plays a crucial part in energy buffering and overall cellular bioenergetics. Several physiological processes can be emphasized in the case of carnitine, including the oxidation of pyruvate and the transport of fatty acids into mitochondria for β-oxidation.[33] Low concentrations of these substances may therefore be interpreted as a sign of mitochondrial dysfunction.

The most prevalent age-related dementia is AD. The prognosis is determined by the change in metabolic parameters. Reduced cerebral glucose uptake is seen in at-risk patients. Furthermore, as people age, type 2 diabetes mellitus raises their risk of AD. The histological diagnosis of AD may therefore be predicted by alterations in glucose uptake in the cerebral cortex. The pathophysiology of AD syndrome is advanced by changes in glucose uptake and metabolism, insulin resistance, oxidative stress, and aberrant autophagy.[34]

One pathological characteristic of AD is impaired cerebral glucose metabolism; new proteomic investigations have shown that AD is associated with disturbed glial metabolism. Inhibition of indoleamine-2,3-dioxygenase 1, which catalyzes the conversion of tryptophan to kynurenine, rescues hippocampal memory function in preclinical mouse models of AD by restoring astrocyte metabolism. In an aryl hydrocarbon receptor-dependent way, amyloid-β and tau oligomers activate astrocytic indoleamine-2,3-dioxygenase 1, which raises kynurenine and inhibits glycolysis. Indoleamine-2,3-dioxygenase 1 inhibition restores hippocampal long-term potentiation and enhances hippocampal glucose metabolism in amyloid and tau models in a monocarboxylate transporter-dependent manner.[35]

5. Conclusion

Four metabolites identified in this study demonstrated strong discriminative power for AD diagnosis, offering a method for detecting biomarkers that could enhance patient diagnosis and prognosis in the future. This study provides new insights into the etiology, early detection, and potential therapy of AD involving blood metabolic biomarkers, warranting further investigation.

Acknowledgments

None.

Funding

None.

Conflict of interest

The authors declare they have no competing interests.

Author contributions

Conceptualization: Maha Z. Rizk, Hanan F. Aly
Formal analysis: Eman A. Younis, Asmaa F. Aboul-Naser
Investigation: Samir H. I. Haggag, Noha S. Hussein, Abdel-Hamid Z. Abdel-Hamid
Methodology: Noha S. Hussein, Samir H. I. Haggag
Writing–original draft: Hanan. Aly and Noha S. Hussein
Writing–review & editing: All authors

Ethics approval and consent to participate

All procedures were designed according to the ethical principles for medical research involving animal subjects. The study protocol was ethically reviewed and approved by the Ethics Review Committee of the National Research Center in Cairo (Approval no: 12010114).

Consent for publication

Not applicable.

Availability of data

Raw data are available from the corresponding author upon reasonable request.

References

1. Armstrong AR. What causes Alzheimer's disease? *Folia Neuropathol*. 2013;51(3):169-188.

   doi: 10.5114/fn.2013.37702

2. Liu Y, Xu S, Bian H, *et al*. Xingnaojing ameliorates synaptic plasticity and memory deficits in an Aβ1-42 induced mouse model of Alzheimer's disease. *J Pharmacol Sci*. 2020;143(4):245-254.

doi: 10.1016/j.jphs.2020.05.002

3. Wang H, Shang Y, Wang E, *et al*. MST1 mediates neuronal loss and cognitive deficits: A novel therapeutic target for Alzheimer's disease. *Prog Neurobiol*. 2022;214:102280.

doi: 10.1016/j.pneurobio.2022.102280

4. Alzahrani AYA, Ullah H, Rahim F, *et al*. Synthesis, biological evaluation and in silico molecular modelling studies of chloro substituted bis-indole containing benzohydrazide analogues as potential anti-diabetic and anti-Alzheimer's agents. *J Mol Struct*. 2024;1316:138908.

doi: 10.1016/j.molstruc.2024.138908

5. Nadeem MS, Shawkat H, Fazal R, *et al*. Synthesis, biological evaluation, molecular docking and dynamic simulation of novel benzofuran derivatives as potential agents against Alzheimer's disease. *J Mol Struct*. 2025;1322:140279.

doi: 10.1016/j.molstruc.2024.140279

6. El-Tallawy HN, Farghly WM, Shehata GA, *et al*. Dementia Prevalence in Kharga District, New Valley Governorate, Egypt. *Neuroepidemiology*. 2012;38(3):130-137.

doi: 10.1159/000335655

7. Dattatray Shinde S, Kumar Behera S, Kulkarni N, *et al*. Bifunctional backbone modified squaramide dipeptides as amyloid beta (Aβ) aggregation inhibitors. *Bioorg Med Chem*. 2024;97:117538.

doi: 10.1016/j.bmc.2023.117538

8. Cai H, Cong WN, Ji S, *et al*. Metabolic dysfunction in Alzheimer's disease and related neurodegenerative disorders. *Curr Alzheimer Res*. 2012;9(1):5-17.

doi: 10.2174/156720512799015064

9. Trushina E, Mielke MM. Recent advances in the application of metabolomics to Alzheimer's Disease. *Biochim Biophys Acta*. 2014;1842(8):1232-1239.

doi: 10.1016/j.bbadis.2013.06.014

10. Snowden MB, Steinman LE, Bryant LL, *et al*. Dementia and co-occurring chronic conditions: a systematic literature review to identify what is known and where are the gaps in the evidence? *Int J Geriatr Psychiatry*. 2017;32(4):357-371.

doi: 10.1002/gps.4652

11. Amidfar M, Askari G, Kim YK. Association of metabolic dysfunction with cognitive decline and Alzheimer's disease: A review of metabolomic evidence. *Prog Neuropsychopharmacol Biol Psychiatry*. 2024;128:110848.

doi: 10.1016/j.pnpbp.2023.110848

12. Vesga-Jiménez DJ, Martin C, Barreto GE, *et al*. Fatty Acids: An Insight into the Pathogenesis of Neurodegenerative Diseases and Therapeutic Potential. *Int J Mol Sci*. 2022;23(5):2577.

doi: 10.3390/ijms23052577

13. Orioli R, Belluti F, Gobbi S, *et al*. Naturally Inspired Coumarin Derivatives in Alzheimer's Disease Drug Discovery: Latest Advances and Current Challenges. *Molecules*. 2024;29(15):3514.

doi: 10.3390/molecules29153514

14. Abd El-Karim SS, Anwar AA, Ahmed NS, Syam YM, *et al*. Discovery of novel benzofuran-based derivatives as acetylcholinesterase inhibitors for the treatment of Alzheimer's disease: Design, synthesis, biological evaluation, molecular docking and 3D-QSAR investigation. *Eur J Med Chem*. 2023;260:115766.

doi: 10.1016/j.ejmech.2023.115766

15. Rizk MZ, Fouad GI, Aly HF, *et al*. Therapeutic impact of a benzofuran derivative on Aluminium chloride-induced Alzheimer's disease-like neurotoxicity in rats via modulating apoptotic and Insulin 1 genes. *Biochem Biophys Res Commun*. 2024;739:150971.

doi: 10.1016/j.bbrc.2024.150971

16. Kamel NN, Aly HF, Fouad GI, *et al*. Anti-Alzheimer activity of new coumarin-based derivatives targeting acetylcholinesterase inhibition. *RSC Adv*. 2023;13(27):18496-18508.

doi: 10.1039/d3ra02344c

17. Inan-Eroglu E, Ayaz A. Is aluminum exposure a risk factor for neurological disorders? *J Res Med Sci*. 2018;23(1):51.

doi: 10.4103/jrms.JRMS_921_17

18. Liaquat L, Sadir S, Batool Z, *et al*. Acute aluminum chloride toxicity revisited: Study on DNA damage and histopathological, biochemical and neurochemical alterations in rat brain. *Life Sci*. 2019;217:202-211.

doi: 10.1016/j.lfs.2018.12.009

19. Abdel Dayem D, Ahmed A, Abdel Hafez S, Gamal El-Tahawy N, Abdel-Aleem S. Possible Effects of Aluminum Chloride Induced Toxicity on Hippocampus of Adult Male Albino Rats. *Minia J Med Res*. 2023;34(4):144-154.

doi: 10.21608/mjmr.2023.215259.1408

20. Ammar NM, Farag MA, Kholeif TE, *et al*. Serum metabolomics reveals the mechanistic role of functional foods and exercise for obesity management in rats. *J Pharm Biomed Anal*. 2017;142:91-101.

doi: 10.1016/j.jpba.2017.05.001

21. Abdoon ASS, Soliman SS, Hussein NS, Haggag SHI, El-Sanea AM, Abdel-Hamid AHZ. Metabolomic profile of dromedary camel follicular fluid during the breeding and non-breeding seasons. *Sci Rep*. 2025;15(1):10452.

doi: 10.1038/s41598-025-91710-9

22. Xia J, Psychogios N, Young N, *et al*. MetaboAnalyst: a web server for metabolomic data analysis and interpretation. *Nucleic Acids Res*. 2009;37(Web Server

issue):W652-W660.

doi: 10.1093/nar/gkp356

23. Hussein NS, S Helmy A, Sherif NM, *et al*. Lipidomic analysis reveals the efficiency of Eclipta prostrata on diet-induced nonalcoholic fatty liver disease in rats. *J Pharm Biomed Anal*. 2019;165:224-232.

doi: 10.1016/j.jpba.2018.11.060

24. Vignoli A, Bellomo G, Paoletti FP, *et al*. Studying Alzheimer's disease through an integrative serum metabolomic and lipoproteomic approach. *J Transl Med*. 2025;23(1):412.

doi: 10.1186/s12967-025-06148-4

25. Yin C, Harms AC, Hankemeier T, *et al*. Status of Metabolomic Measurement for Insights in Alzheimer's disease Progression-What Is Missing? *Int J Mol Sci*. 2023;24(5):4960.

doi: 10.3390/ijms24054960

26. Mesa-Herrera F, Taoro-González L, Valdés-Baizabal C, Diaz M, Marín R. Lipid and Lipid Raft Alteration in Aging and Neurodegenerative Diseases: A Window for the Development of New Biomarkers. *Int J Mol Sci*. 2019;20(15):3810.

doi: 10.3390/ijms20153810

27. Kanfer JN, Pettegrew JW, Moossy J, *et al*. Alterations of selected enzymes of phospholipid metabolism in Alzheimer's disease brain tissue as compared to non-Alzheimer's demented controls. *Neurochem Res*. 1993;18(3):331-334.

doi: 10.1007/BF00969091

28. Walter A, Korth U, Hilgert M, *et al*. Glycerophosphocholine is elevated in cerebrospinal fluid of Alzheimer patients. *Neurobiol Aging*. 2004;25(10):1299-1303.

doi: 10.1016/j.neurobiolaging.2004.02.016

29. Martínez M, Mougan I. Fatty acid composition of human brain phospholipids during normal development. *J Neurochem*. 1998;71(6):2528-2533.

doi: 10.1046/j.1471-4159.1998.71062528.x

30. González-Domínguez R, García-Barrera T, Gómez-Ariza JL. Metabolomic study of lipids in serum for biomarker discovery in Alzheimer's disease using direct infusion mass spectrometry. *J Pharm Biomed Anal*. 2014;98:321-326.

doi: 10.1016/j.jpba.2014.05.023

31. García-Cruz VM, Arias C. Palmitic Acid Induces Posttranslational Modifications of Tau Protein in Alzheimer's Disease-Related Epitopes and Increases Intraneuronal Tau Levels. *Mol Neurobiol*. 2024;61(8):5129-5141.

doi: 10.1007/s12035-023-03886-8

32. Mosconi L, Mistur R, Switalski R, *et al*. FDG-PET changes in brain glucose metabolism from normal cognition to pathologically verified Alzheimer's disease. *Eur J Nucl Med Mol Imaging*. 2009;36(5):811-822.

doi: 10.1007/s00259-008-1039-z

33. Adhihetty PJ, Beal MF. Creatine and its potential therapeutic value for targeting cellular energy impairment in neurodegenerative diseases. *Neuromolecular Med*. 2008;10(4):275-290.

doi: 10.1007/s12017-008-8053-y

34. Kumar V, Kim SH, Bishayee K. Dysfunctional Glucose Metabolism in Alzheimer's disease Onset and Potential Pharmacological Interventions. *Int J Mol Sci*. 2022;23(17):9540.

doi: 10.3390/ijms23179540

35. Minhas PS, Jones JR, Latif-Hernandez A, *et al*. Restoring hippocampal glucose metabolism rescues cognition across Alzheimer's disease pathologies. *Science*. 2024;385(6711):eabm6131.

doi: 10.1126/science.abm6131